Thermal conductivity of thin films: Measurements and understanding

David G. Cahill, Henry E. Fischer, Tom Klitsner, E. T. Swartz, and R. O. Pohl

Citation: Journal of Vacuum Science & Technology A: Vacuum, Surfaces, and Films **7**, 1259 (1989);
View online: https://doi.org/10.1116/1.576265
View Table of Contents: http://avs.scitation.org/toc/jva/7/3
Published by the American Vacuum Society

Thermal conductivity of thin films: Measurements and understanding

David G. Cahill, Henry E. Fischer, Tom Klitsner,[a] E. T. Swartz,[b] and R. O. Pohl
Laboratory of Atomic and Solid State Physics, Cornell University, Ithaca, New York 14853-2501

(Received 19 August 1988; accepted 10 October 1988)

Several techniques are reviewed with which thermal conductivity and phonon scattering can be measured in films of thicknesses ranging from angstroms to millimeters. Recent experimental results are compared critically with previous measurements. It is shown that phonons are very sensitive probes of the structural perfection of the films.

I. INTRODUCTION

Depending on the way thin films have been deposited onto a substrate, they will contain various degrees of disorder. This disorder will influence the thermal conductivity of the films, and thus the heat removal from them. Conversely, measurements of the thermal conductivity can lead to a better understanding of the disorder in such films. In this paper, we will review several measuring techniques which have been recently developed and used at Cornell to study films of a wide range of thicknesses. One is an ac technique which can be used to measure the thermal conductivity and specific heat of films 10 μm and thicker. The second technique is a dc technique developed to measure the heat transport across interfaces, but it is also sensitive to the thermal conductivity of thin films, and is particularly useful for films thinner than 1 μm. Both techniques can also be used to test the quality of the bonding to the substrate with a high spatial resolution. The third technique takes advantage of the phenomenon that the elastic waves or phonons which carry the heat in a substrate are sensitive to the properties of the surface, and can thus be used to probe adsorbed atoms or thin films with average thicknesses of a few angstroms and up.

In addition to probing different film thicknesses with these techniques, we can also change the length scale on which we are probing the films; this is done by varying the temperature of the measurement, and therefore the wavelengths of the phonons involved in the heat flow.

The widely recognized need for thermal data on thin films is demonstrated by the large number of publications on various methods to measure their thermal diffusivity, thermal conductivity, and specific heat, although these experimental data are still scant. This brief review cannot do justice to all these efforts. Instead we will restrict ourselves to occasional comparisons with results obtained by other researchers, and refer the interested reader to some recent publications in the field.[1-4]

II. 3-ω TECHNIQUE FOR FILMS TENS OF μm THICK

This ac technique was developed[5] mainly because of its insensitivity to radiative heat losses and has been used to measure the thermal conductivity of bulk glasses below room temperature, and in some cases up to as high as 750 K.[6]

A thin, evaporated metal strip with four pads to measure current and voltage, see Fig. 1, is used as a heater and also as a thermometer, because of the temperature-dependent electrical resistance of the metal strip. An ac current with (angular) frequency ω will cause a temperature wave of frequency 2ω to diffuse into the substrate. This wave has cylindrical symmetry, and is exponentially damped in the radial direction, see the insert in Fig. 2. Its wavelength, or more precisely its penetration depth $|q^{-1}|$, is given by

$$|q^{-1}| = (D/2\omega)^{1/2}, \tag{1}$$

where D is the thermal diffusivity, $D = \Lambda/C_p$ where Λ is the thermal conductivity, and C_p the specific heat per volume. The temperature amplitude ΔT of the heater is inversely proportional to the thermal conductivity of the substrate and to the logarithm of the reciprocal angular frequency ω^{-1}. By measuring ΔT as a function of ω, Λ can be directly determined without having to determine C_p. The 3ω technique probes the sample to a depth of the order of $|q^{-1}|$, which varies typically between 10^{-3} and 10^{-5} m, depending on ω (and D). It has been used to measure the thermal conductivity of a variety of solids, and has thus been tested.

By increasing the frequency ω, the technique can be adapted to measuring the thermal conductivity of the near-surface region, or of films on substrates. If the heater/thermometer is evaporated onto a dielectric film of thickness d, situated on some substrate (see inset of Fig. 2), the temperature wave will be confined to the film if $|q^{-1}| < d$. If, however, $|q^{-1}| \gg d$, the film can be neglected, and the temperature wave can be considered as diffusing entirely in the substrate. The temperature amplitude ΔT as a function of the frequency of the temperature oscillation (which is $2\omega/2\pi$) is shown in Fig. 2 for an amorphous silicon film adhering to an alumi-

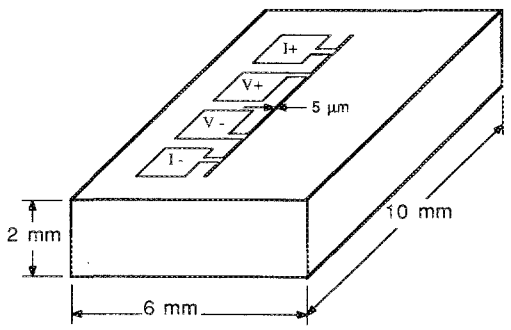

FIG. 1. Evaporated metal pattern produced on the face of a sample used for the 3ω technique. The four pads are the connections for current leads I^+, I^- and voltage leads, V^+, V^-. The narrow metal line that serves as the heater and thermometer for the measurement of the thermal conductivity is at the center of the face of the sample. The patterns made by photolithography; linewidth is 5 μm; length typically 1 mm.

 0734-2101/89/031259-08$01.00

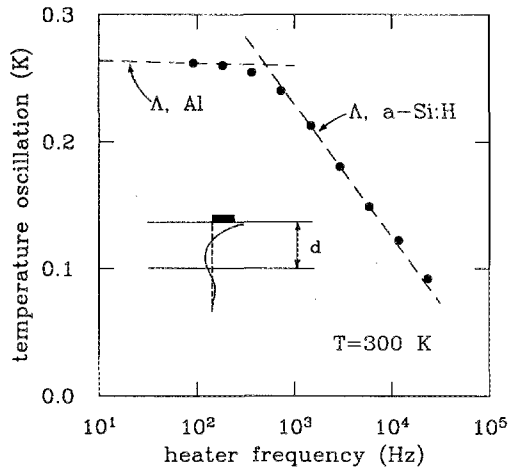

FIG. 2. Data analysis for the 3ω technque. Example of the amplitude of temperature oscillation of the heater/thermometer for a 25-μm-thick film of hydrogenated a-Si on an aluminum substrate, as a function of the frequency of the temperature oscillation ($2\omega/2\pi$). For $2\omega > 2\pi 10^3$ rad s^{-1}, the penetration depth is less than d, the thickness of the a-Si:H film (25 μm). From the slope of the dotted line, the thermal conductivity can be determined. For $2\omega < 2\pi 10^3$ rad s^{-1}, the penetration depth exceeds d, and the slope of the dotted line is determined by the thermal conductivity of the substrate. Inset: Use of the 3ω method for measurements of films with thicknesses d as small as ~ 10 μm. The exponentially damped curve shows a snapshot temperature profile at the instant when the temperature at the heater is at a maximum. The penetration depth $|q^{-1}|$ defined in the text is about two-thirds the distance between heater and the intersection of this temperature profile and the $\Delta T = 0$ line (dashed). By choosing the ac heater current angular frequency ω large enough, the penetration depth can be made $\ll d$, in which case the thermal conductivity of the film is measured.

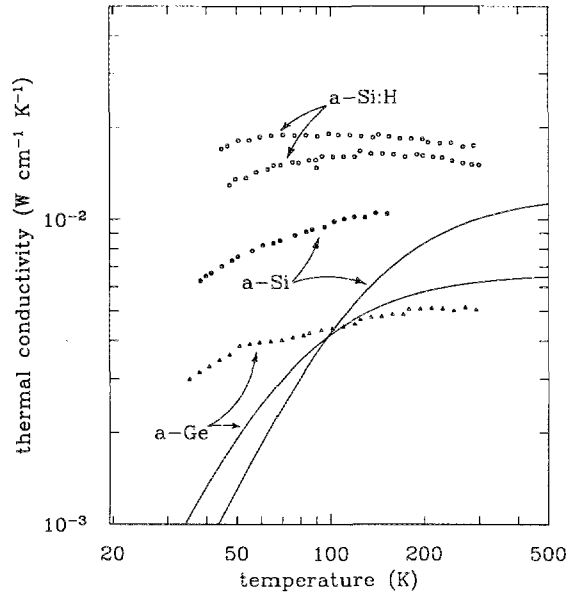

FIG. 3. Thermal conductivity of ~ 50-μm-thick films of a-Si, a-Ge, and a-Si:H (20%) between 30 and 300 K as measured with the 3ω technique. The solid curves are the minimum thermal conductivities for a-Ge and a-Si, respectively, based on Slack's proposal (Ref. 8).

num substrate. For small frequencies, the small slope of the straight line obtained when ΔT is plotted versus the natural logarithm of this frequency is the result of the large thermal conductivity of the aluminum (obviously, the frequency range is inadequate to measure Λ in this case). As the frequency increases beyond $\sim 10^3$ Hz, ΔT decreases rapidly, and approaches a straight line in Fig. 2, from which the thermal conductivity of the a-Si can be determined. By repeating this measurement at different temperatures, $\Lambda(T)$ can be determined. It should be emphasized that the success of this technique depends on good bonding between film and substrate. Consequently, these measurements can also reveal flaws in the bonding with a spatial resolution given by the length of the metal film heater/thermometer, which is of the order of 1 mm (see Fig. 1). This potential application of this measuring technique has not yet been pursued.

Examples of experimental results obtained with this technique are shown in Fig. 3. The a-Ge and a-Si films had been produced by sputtering and were kindly supplied by Dr. S. Moss (now at the University of Houston, then at Energy Conversion Devices, ECD) and Dr. J. Lannin (Penn State). The hydrogenated a-Si films (20 mol % hydrogen) were produced by chemical vapor deposition on aluminum substrates at 250 °C by Dr. J. Mort (Xerox Webster Labs). The thermal conductivities of the films in Fig. 3 have been compared to a theoretical prediction based on a model first used by Einstein[7] as refined by Slack.[8] It is based on the assumption that neighboring atoms or groups of atoms vibrate with random phases (the opposite, i.e., nonrandom phases will lead to elastic waves). It has recently been shown[5] that in bulk amorphous solids the measured thermal conductivity above 50–100 K, and up to the softening point, is well described through this model, i.e., through a random walk of the elastic energy (i.e., heat) from one localized (Einstein) oscillator to the next. In terms of the model of the minimum thermal conductivity considered by Slack,[8] we found that the data for glasses were best described by a phonon mean free path equal to one-half the phonon wavelength (while Slack proposed a mean free path twice as long). Our measurements on a-Ge and a-Si films agree well with the numerical calculation based on this model and indicate that these films behave like bulk amorphous material. Interestingly, however, in hydrogenated silicon films, the thermal conductivity is distinctly larger than in pure a-Si. This observation shows that the thermal conductivity of these amorphous films is not independent of doping or perhaps of preparation, in contrast to bulk glasses. The cause is not understood.

A comparison with earlier results for a-Ge is shown in Fig. 4: Nath and Chopra[9] measured the thermal conductivity between 100 and 500 K of films of Ge, 0.2–0.8 μm thick, produced by thermal evaporation onto mica sheets, and found it to be independent of thickness. Yet, for a-Ge, they found thermal conductivities one order of magnitude larger than our values, and approaching those for polycrystalline films at 500 K. Goldsmid and Paul[10] measured a film 1.12 μm thick, produced by thermal evaporation onto sapphire, and found an intermediate value for the thermal conductivity, see Fig. 4. Using the 3ω technique, another tetrahedrally coordinated glass $CdGeAs_2$, which is available in bulk form, has recently been measured,[11] see Fig. 4. Its thermal conductivity agrees closely with our results on a-Ge films, as expected on the basis of Slack's model because of the similarity in structure and the speed of sound in these solids. This agreement can be taken as evidence that our experimental results

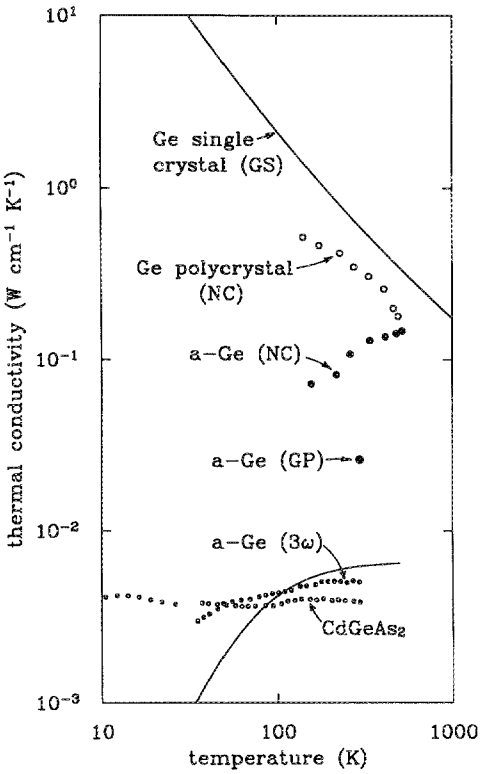

FIG. 4. Comparison of the thermal conductivities of films of *a*-Ge from different studies. NC: Nath and Chopra, Ref. 9, 0.7 μm thick; GP: Goldsmid and Paul, Ref. 10, 1.2 μm thick. 3ω: This investigation, same data and same theoretical prediction as in Fig. 3; Cd Ge As_2: amorphous bulk material (Ref. 11). Also shown is the thermal conductivity of single-crystal Ge [GS: C. J. Glassbrenner and G. A. Slack, Phys. Rev. A **134**, 1058 (1964)], and of a polycrystalline Ge film, 0.9 μm thick (NC:Ref. 9).

on the *a*-Ge film are indeed those of bulk, amorphous germanium.

Using two slightly different techniques, Goldsmid and coworkers measured at room temperature two films of *a*-Si of 1.2-μm thickness evaporated onto crystalline Al_2O_3 (Ref. 12) and Si.[13] They reported 2.6×10^{-2} and 4.2×10^{-2} W cm^{-1} K^{-1}, respectively, while our data extrapolate to 10^{-2} W cm^{-1} K^{-1} at 300 K.

It is difficult to determine the cause of these discrepancies. Can amorphous films of micrometer thickness have much larger thermal conductivities than the same material in bulk form? This question will be addressed in the following section.

III. THERMAL CONDUCTIVITY OF THIN FILMS IN THE μm RANGE

For films $< 10\,\mu$m thick the frequencies ω needed to satisfy Eq. (1) quickly become cumbersome because of the required lock-in techniques, and thus the 3ω technique becomes less suitable. The technique through which the thermal conductivity of films even thinner than 100 Å can be measured was originally developed[14] to measure the thermal boundary resistance that produces a temperature drop at the interface between two solids across which heat is flowing. Figure 5 shows the experimental geometry.[15] Two closely spaced ($\sim 2\,\mu$m) narrow metal strips are vapor deposited onto a dielectric substrate. The interface that is studied is

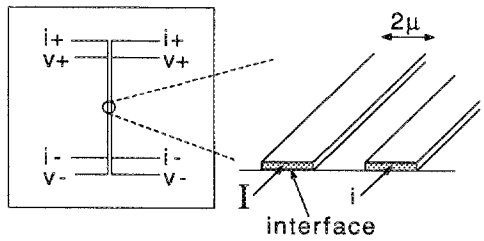

FIG. 5. Experimental geometry for measuring thermal boundary resistance and also the thermal resistance of films in the μm thickness range. The heater/thermometer lines are typically 2.5 mm long. The substrate is typically a plate $1\times1\times0.025$ cm^3. The interface studied is that between the left metal strip and substrate. To measure the thermal conductivity of thin dielectric films, they would be deposited on the substrate before depositing the metal films (Ref. 14).

between one metal strip and the substrate underneath it. Through that strip, a relatively large sensing current I is used to measure the resistance R and thus the temperature of that strip; $\dot{Q} = I^2R$ causes that temperature to be larger than the temperature of the underlying substrate. The temperature of the second thermometer strip is determined by measuring its resistance using a much smaller sensing current i, to avoid self-heating. The difference between the temperature of the second thermometer and the temperature of the substrate underneath the first thermometer is calculated by integrating the time-independent heat diffusion equation for the geometry of Fig. 5; this temperature difference is a small correction because of the smallness of the separation of the thermometers, and because of the large thermal conductivity of the Al_2O_3 substrate.

The thermal boundary resistance between the Joule heated thermometer and the underlying substrate is given by the ratio of the temperature difference ΔT between the strip and the substrate, and the power per unit area $\dot{Q}/A$ flowing across the interface:

$$R_{bd} = \frac{\Delta T}{\dot{Q}/A}. \tag{2}$$

The thermal resistance between a film of rhodium (doped with iron to increase its sensitivity as a resistance thermometer at low temperature) and a polished sapphire crystal substrate is shown in Fig. 6 (see the symbols $\times$). Below ~ 20 K, the data agree well with the theoretical prediction (see the solid line) based on the assumption that the mismatch in the acoustic impedances of the solids will limit the fraction of the elastic waves (and therefore the heat) that will be transmitted across the interfaces, the rest being reflected. This model is called the acoustic mismatch model (AMM) and was first proposed by Khalatnikov[16] and independently by Mazo[17] to explain the thermal boundary resistance between liquid helium and solids (the Kapitza resistance). It should also be mentioned, however, that the theoretical prediction of R_{bd} for the data shown in Fig. 6 will change by $< 10\%$ if one assumes that all incident phonons are diffusely scattered at the interface. This assumption is the basis of the diffuse mismatch model (DMM).[15] Above ~ 50 K, however, the experimental thermal boundary resistance exceeds the theoretical one by nearly one order of magnitude for either model. It has been concluded that this discrepancy could

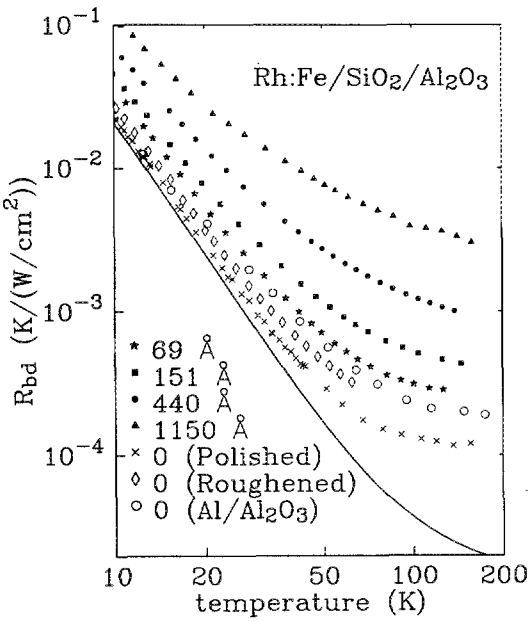

FIG. 6. Effective thermal boundary resistances for Rh:Fe/Al_2O_3 interfaces with interlayers of a-SiO_2, with a damaged layer at the interface resulting from a diamond polish (◊), and for an argon ion-bombarded Al/Al_2O_3 interface (○). The solid curve represents diffuse mismatch theory for an undamaged Rh:Fe/Al_2O_3 interface without a glassy interlayer, but is practically identical for the case of acoustic mismatch, and even for an Al/Al_2O_3 interface (Ref. 15).

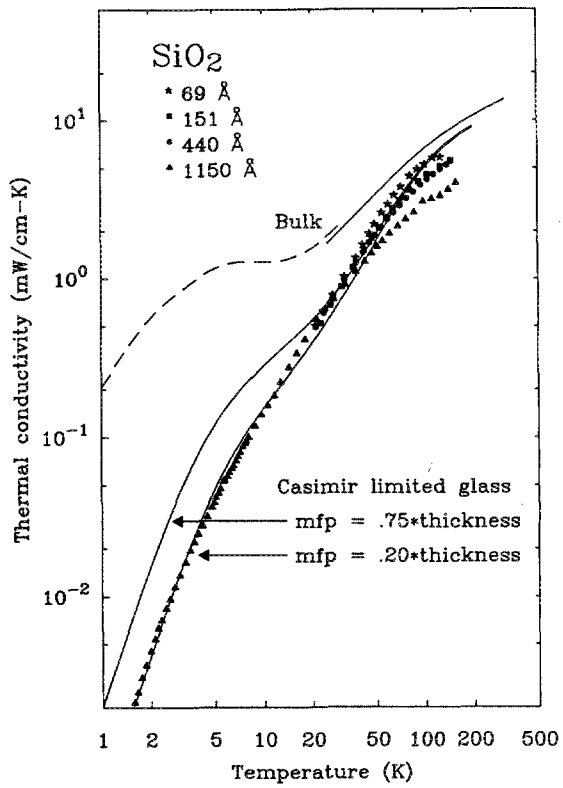

FIG. 7. Effective thermal conductivity of thin glass films after Ref. 14. The dashed curve represents the thermal conductivity data for bulk a-SiO_2 (Vitreosil) by Raychaudhuri and Pohl, Ref. 18, and the upper solid curve represents the data of Cahill and Pohl (Ref. 5). The curves called Casimir limited glasses were computed with a Debye thermal conductivity integral by assuming a phonon wavelength independent scattering mean free path (mfp) of the magnitude indicated, in addition to the mean free path needed to describe the conductivity of the bulk glass.

neither be blamed on details of the calculation, nor on the experimental method.[14,15] The most likely reason has been proposed to be that the excess thermal resistance was caused by phonon scattering in a thin disordered layer in the substrate close to the interface. This was confirmed by the observation that the same metal film on an Al_2O_3 surface roughened with 2000-Å diamond polish resulted in an increased R_{bd} (see Fig. 6). An even larger R_{bd}, predominantly above 30 K, was observed when an Al film was deposited while argon-ion bombarding the sapphire surface before and during the first 10 Å of deposition, shown as the open circles.

In order to quantify the disorder produced scattering somewhat better, thin a-SiO_2 layers were deposited (by plasma enhanced chemical vapor deposition) on the polished sapphire surface before depositing (by magnetron sputtering) the Rh:Fe films. (Note that this arrangement resembles one developed by Goldsmid and co-workers[12,13] to measure 1.2-μm-thick a-Ge and a-Si films mentioned earlier.) The resistance of this assemblage, called an effective boundary resistance, is also shown in Fig. 6. In Fig. 7 we compare the thermal conductivities of the a-SiO_2 layer, derived from these measurements, with the thermal conductivity of bulk a-SiO_2,[5,18] and find it to be much smaller, see Fig. 7. The two solid curves in Fig. 7 were computed with the assumption that the phonons in the 1150-Å-thick film are being scattered by an additional, wavelength-independent scattering mechanism. Such scattering can conceivably occur at the two surfaces of the film; however, the phonon mean free path (mfp) required to fit the low-temperature data is five times shorter than the film thickness. This suggests the existence of macroscopic flaws within the film, which leads to the wavelength-independent scattering. However, above ~100 K, the thermal conductivity of the film is still smaller than can be explained by such a scattering mechanism. We mentioned in the preceding section that in glasses above ~50 K the heat is carried by a random walk of the elastic energy between neighboring localized (Einstein) oscillators. In such a situation, the thermal conductivity can only be lowered if the glass is porous so that the pathway for the diffusion is increased. Thus we conclude that the a-SiO_2 films used in these experiments, in particular, the thick ones, are somehow porous. No independent microscopic studies of our a-SiO_2 films have been performed, although it is well known that thick a-SiO_2 films can have such flaws.[19] For the purpose of the present discussion, it suffices to say that the thermal conductivity measurements of these films point to significant macroscopic flaws, which lead to greatly reduced heat carrying capabilities. No evidence for an enhancement of the conductivity is observed, contrasting to the evidence presented for micrometer-sized films of a-Ge and a-Si in the previous section.

This technique should also be very sensitive to the quality of the bond between film and substrate. It has been observed that the thermal boundary resistance between gold and sapphire is three times larger than expected for either diffuse or acoustic mismatch.[14] Since gold adheres only weakly to sapphire (it can easily be wiped off), it has been suggested that

this enhanced resistance is an indication for imperfect bonding between these two solids.

IV. PHONON SCATTERING IN FILMS WITH THICKNESSES IN THE NANOMETER RANGE

We have seen in the preceding section that some macroscopic disorder can lead to a significant reduction of the thermal conductivity of thin films relative to that observed in bulk material. In this section we will study the phonon scattering in these films not through measurements of their thermal conductivity, but by observing the probability of diffuse scattering of phonons from within the substrate impinging onto the surface supporting the film. First, we measure the thermal conductivity of high-purity samples of single-crystal material with polished surfaces in the temperature regime in which bulk scattering of the phonons is negligible, and the phonons fly ballistically between collisions with the sample surfaces. In this radiative, or Casimir limit,[20,21] the thermal conductivity will increase as the probability f for diffuse scattering events at the surfaces decreases. (Strictly speaking, one should not talk about thermal conductivity in this case; thermal conductance is more appropriate, since the heat flow is determined not only by the geometry of the sample, but also by the spacing and size of the heater and the thermometers used to perform the measurements, in addition to f. We will ignore this terminology here,[22] although our analysis takes these effects into account.)

The natural way to study this diffuse scattering would be through reflection of heat pulses or monochromatic phonon beams. In fact, such studies are underway in several laboratories.[23–26] The advantage of using thermal conductivity measurements is that the phonons are scattered repeatedly at the surface as they fly along the crystal, and this multiple scattering enhances the sensitivity.

Experimental thermal conductivity results are shown in Fig. 8.[27] The lowest, solid curve is the thermal conductivity between 0.1 and 100 K of a highly perfect silicon crystal with roughened (sandblasted) surfaces. The wavelengths of the elastic waves carrying the bulk of the heat at a given temperature are shown in the upper abscissa. Note that at 1 K, the frequency of these dominant phonons is 90 GHz. This frequency varies linearly with the temperature. The frequencies used in these experiments are therefore relatively small in comparison to the oscillations excited around room temperature, where most of the experiments were done which we have discussed so far. Above the thermal conductivity maximum, near 10 K, the phonons are scattered predominantly in the bulk. Below 10 K, the thermal phonons travel virtually uninhibited between collisions with the walls, which are always diffuse ($f = 1$) because the surfaces are rough. In this case, the phonon mean free path l is given by the sample diameter, and the thermal conductivity Λ

$$\Lambda = \tfrac{1}{3} C_p v l \qquad (3)$$

varies as the third power of the temperature, since the specific heat C_p varies as T^3 (v is an average speed of sound.) If the crystal surfaces are polished (with Syton as the final step) and subsequently cleaned, the thermal conductivity below a few K is greatly enhanced (upper solid curve in Fig. 8), giving evidence for a significant reduction in f, the probability for diffuse scattering. If onto such polished crystal faces,

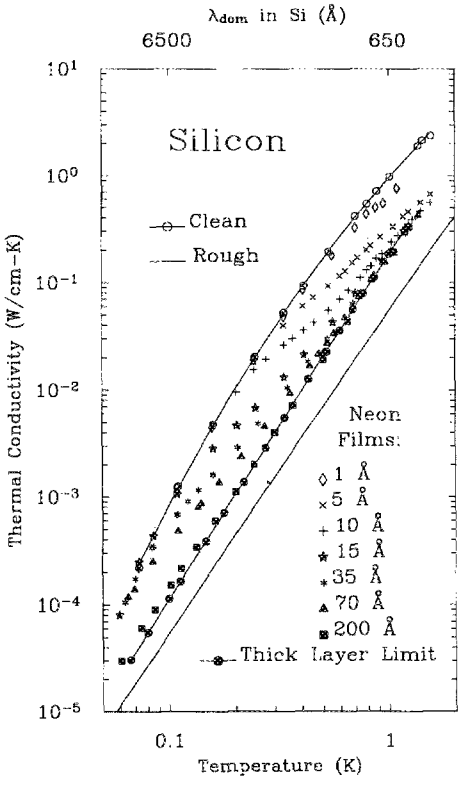

FIG. 8. Thermal conductivity of a Syton polished, clean silicon single crystal (upper curve O) with heat flow along the ⟨111⟩ direction, $5\times5\times50$ mm^3, and of the same sample after *in situ* deposition of neon films of average thickness as indicated (Ref. 27). The lowest curve is the thermal conductivity of a clean sample after surface roughening through sandblasting.

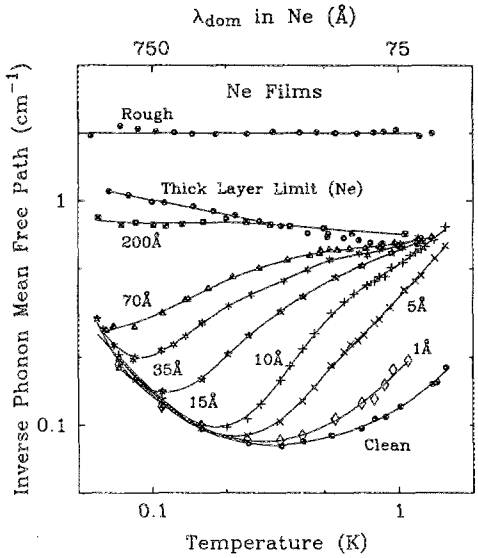

FIG. 9. Experimental inverse phonon mean free path l^{-1} [see Eq. (3)] for different coverages of Ne on Si held at 1 K during the deposition from the gas phase. Even submonolayer coverage (average thickness) leads to a noticeable enhancement of the diffuse scattering. The scattering then increases continuously with increasing coverage until it reaches the thick layer limit. Above this coverage, the scattering becomes independent of the film thickness. The transition from specular reflection to diffuse scattering as the temperature increases is clearly visible for all coverages (Ref. 27).

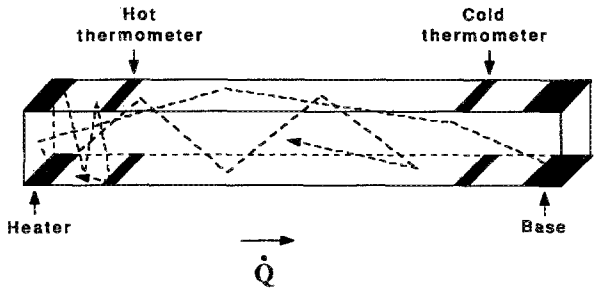

FIG. 10. Thermal conductivity measurement of a substrate crystal with the positions of the clamps for heater, thermometers, and heat sink (base) indicated by crosshatching; $\dot{Q}$ indicates the heat flow. In our experiments, the substrate is a ⟨111⟩ Si crystal with Syton polished and cleaned surfaces, $5\times5\times50$ mm^3. The dashed lines show some paths of the phonons as simulated in the Monte Carlo calculation (Ref. 22). Specular reflection does not lead to a thermal resistance.

thin films of neon are condensed *in situ*, at low temperature and under high vacuum (with the average film thickness determined with a silicon paddle oscillator[27]) the thermal conductivity is reduced as shown in Fig. 8. The thickest films, 200 Å and thicker (up to 1 μm, the so-called thick layer limit), produce a thermal conductivity with almost the same temperature dependence as produced by boundary scattering for a rough sample ($\propto T^3$, Casimir[20]). The wavelength-independent phonon mean free path, however, is two to three times larger than in the Casimir case. Films with average film thickness smaller than the thick layer limit do not scatter the long-wavelength phonons carrying the heat below $\sim$1 K, but do scatter the short-wavelength ones. The transition between weak scattering and strong scattering shifts to lower temperatures with increasing film thickness, and seems to occur when the phonon wavelength in the film exceeds its thickness. Under those conditions, the phonons apparently are less likely to be scattered. This transition between weak and strong scattering is shown even more clearly in Fig. 9 in which the reciprocal phonon mean free path l^{-1} as defined in Eq. (3), and which is proportional to a scattering rate, is plotted for the data shown in Fig. 8.

In order to quantify the scattering by the neon films, we have determined f, the probability of diffuse scattering for the coated samples, and subtracted from that the residual probability for the clean, polished silicon sample. The probability f was determined using a Monte Carlo calculation for a geometry representing the thermal conductivity sample, see Fig. 10. This method was developed by one of us (H.E.F.), and is described in detail in Ref. 22. Quanta of heat (phonons) are injected into the sample at the heater and are followed by the computer as they bounce along the sample on their way towards the heat sink at the base. The number of particles hitting the crosshatched areas marking the position of the thermometers can be translated into a phonon flux, and thus a temperature. By performing simulations with different f, we can simulate the experimentally observed temperature drops between the two thermometers and can make quantitative comparisons between simulation and experiment. With this procedure, the probability f for diffuse scattering by the neon films has been determined, see Fig. 11. It increases with increasing film thickness, up to a limiting value $f_{max}\sim0.3$. Only the very thickest films show evidence for even larger scattering probability. The explanation proposed is that the phonons must enter the films in order to be scattered, and once they have entered they are inevitably scattered either within the neon film, or at its free surface. Thus f is determined solely by the probability of the phonons entering the films. This latter probability has been calculated us-

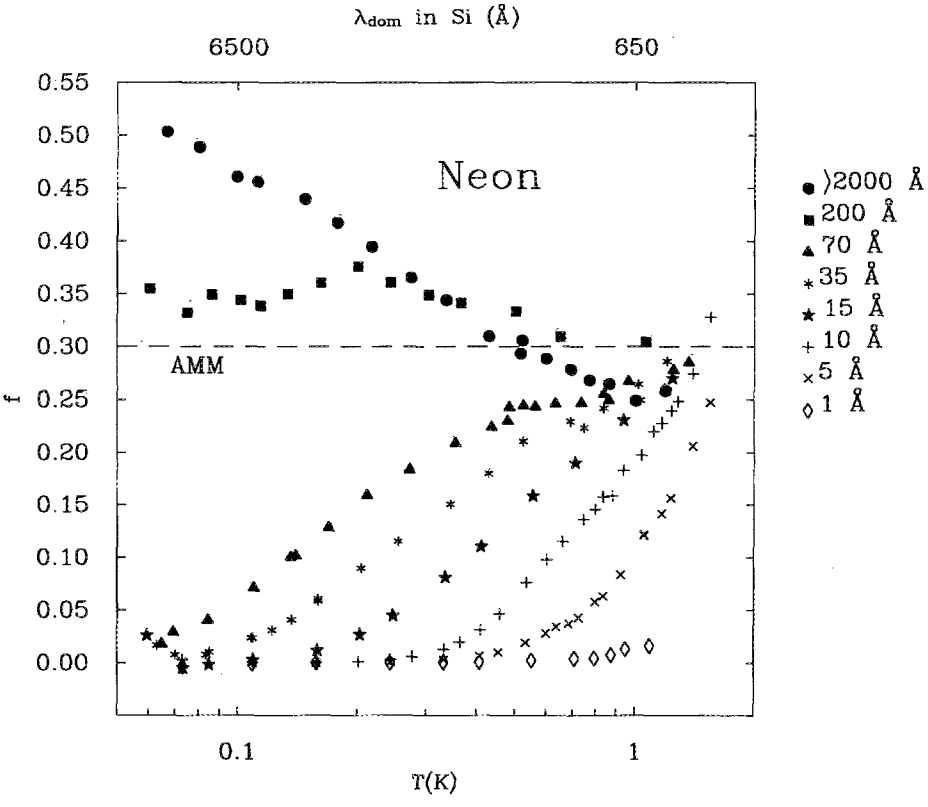

FIG. 11. Probability f for diffuse scattering resulting from neon films of different average thickness. The data are the same as those shown in Figs. 8 and 9. At film thicknesses >2000 Å, f is independent of the film thickness (the "thick layer limit") up to the maximum thickness measured: $\sim$ 1 μm. The dashed line labeled AMM makes the assumptions that the phonon transmission probability into the film is determined by the acoustic mismatch between neon and silicon, and that all phonons thus entering the films will be diffusely scattered.

ing the acoustic mismatch model introduced above, and using the elastic constants of dense, polycrystalline, bulk solid neon for the thick films,[28] which are probably continuous. The calculation shows that only 30% of the incident phonons can enter the thick film and be scattered, leading to $f = 0.3$ as shown with the dashed line marked AMM, in agreement with the experiment (Fig. 11).

As a further test of this picture, the same measurements were performed with hydrogen and deuterium condensed on the polished clean silicon surface. Qualitatively identical results were obtained, except that these films scattered phonons less than neon. The diffuse scattering probability f determined for the thickest films are compared in Fig. 12 with the acoustic mismatch model. Although the agreement is not perfect, the trend is certainly as predicted by this model.

The silicon–frozen gas interface can hardly be viewed as ideal; the clean Si surface carries defects and residual impurities, and the gas atoms must be expected to be deposited randomly during the quenched condensation process. Therefore, one might expect that the phonons will be scattered diffusely at the interface. In this case, f might approach unity for all three gases. Clearly, the experiments disagree with this model, and we conclude that diffuse scattering at the interface is very small. Rather, the transmission is determined by acoustic mismatch, and the scattering must occur within the films. That scattering is amazingly strong, however. Consider the 200-Å Ne film in Fig. 11. Apparently all phonons which enter the film are scattered as they travel back and forth, a distance of a few hundred angstroms. Such strong scattering requires either macroscopic defects, like voids or cracks. It could, however, also result from a rough outer surface of the film. Nothing is known about the structure of such condensed gas films, and thus these phonon experiments give the first evidence about their disorder.

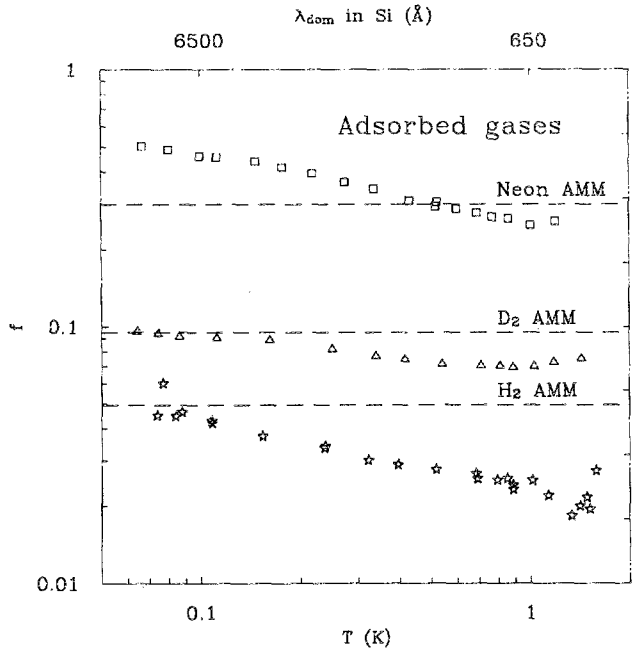

FIG. 12. Diffuse scattering for films of neon, deuterium, and hydrogen condensed at low temperatures on polished Si surfaces in the thick layer limit. Data taken from Ref. 27. The neon data are the same as those shown in Fig. 11 (●).

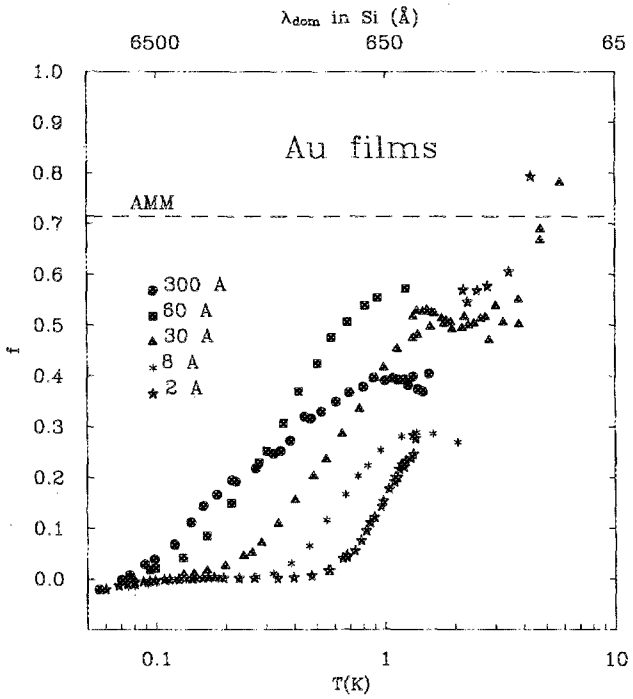

FIG. 13. Diffuse scattering probability resulting from gold films of average thickness as indicated. The line labeled AMM is explained in the text. The measurements are from Ref. 27.

Similar results have been obtained for evaporated gold films on silicon.[27] Figure 13 shows $f(T)$ obtained from a Monte Carlo simulation calculation for average thicknesses varying from 2 to 300 Å. Scanning electron microscope pictures showed the 30- and 60-Å-thick films to consist of discontinuous islands with average diameters of 200 and 400 Å, respectively. The even thinner films were almost certainly also discontinuous, although they could not be studied with the microscope because of inadequate contrast as a result of the low coverage of gold. The 300-Å film was continuous, though cracked like dry mud flats. It has been suggested[27] that the islands act as scattering centers and cause Rayleigh scattering for long wavelengths, and geometric scattering for short ones (compared to the island diameter). In the thick films, the phonons are scattered either by the cracks, or by a roughness (waviness) of the outer surface of the evaporated films. The fact that the experimental f stays below the f calculated from the acoustic mismatch (AMM) may indicate that the disorder is less than in the condensed gas films, but it may also result from incomplete wetting of the silicon by the gold. The latter case would be particularly interesting, since we expect that phonons would be particularly sensitive probes of contacts on the atomic scale.

V. CONCLUSIONS

Measurements of thermal conductivity and of phonon scattering provide sensitive probes for the study of disorder in thin solid films. Different techniques can be used to cover average film thicknesses from angstroms to tens of μm (or thicker). Considerable microscopic disorder appears to exist in many of the films investigated, but details of the scattering mechanisms are still poorly understood. It is safe to say, however, that the thermal conductivities of thin amorphous

and crystalline films can differ significantly from those measured for the bulk materials.

ACKNOWLEDGMENTS

The work reviewed in this paper was supported by the Semiconductor Research Corporation at Cornell, Contract No. 87-01-069, the Cornell Materials Science Center, and the National Science Foundation Grant No. DMR-8714788.

[a] Present address: Sandia National Laboratory, Albuquerque, NM 87185.
[b] Present address: RMC, Inc., 1802 W. Grant Road, Suite 122, Tucson, AZ 85745.

[1]W. P. Leung and A. C. Tam, Appl. Phys. Lett. **51**, 2085 (1987); J. Appl. Phys. **63**, 4505 (1988).
[2]R. E. Taylor and K. D. Maglic, in *Compendium of Thermophysical Property Measurement Methods*, edited by K. D. Maglic, A. Cezairliyan, and V. E.Peletsky (Plenum, New York, 1984), Vol. 1, p. 305; R. E. Taylor, High Temp. High Pressures **15**, 299 (1983).
[3]N. Tsutsumi and T. Kiyotsukuri, Appl. Phys. Lett. **52**, 442 (1988).
[4]L. Wieczorek, G. L. Paul, and H. J. Goldsmid, in *Thermal Conductivity 19*, edited by D. W. Yarbrough (Plenum, New York, 1988), p. 413, also D. Ristau and J. Ebert, Appl. Opt. **25**, 4571 (1986).
[5]D. G. Cahill and R. O. Pohl, Phys. Rev. B **35**, 4067 (1987).
[6]D. G. Cahill (unpublished results).
[7]A. Einstein, Ann. Phys. **35**, 679 (1911).
[8]G. A. Slack, in *Solid State Physics*, edited by F. Seitz and D. Turnbull (Academic, New York, 1979), Vol. 34, p. 1.
[9]P. Nath and K. L. Chopra, Phys. Rev. B **10**, 3412 (1974).
[10]H. J. Goldsmid and G. L. Paul, Thin Solid Films **103**, L47 (1983).
[11]D. G. Cahill and R. O. Pohl, Phys. Rev. B **37**, 8773 (1988).
[12]H. J. Goldsmid, M. M. Kaila, and G. L. Paul, Phys. Status Solidi A **76**, K31 (1983).
[13]L. Wieczorek, H. J. Goldsmid, and G. L. Paul, in *Thermal Conductivity 20*, (Plenum, New York, to be published).
[14]E. T. Swartz, Ph.D. thesis, Cornell Materials Science Center Report No. 6489, 1987.
[15]E. T. Swartz and R. O. Pohl, Appl. Phys. Lett. **51**, 2200 (1987).
[16]I. M. Khalatnikov, J. Exp. Theoret. Phys. (USSR) **22**, 687 (1952); also in *An Introduction to the Theory of Superconductivity*, edited by I. M. Kapitza (Benjamin, New York, 1965), p. 138.
[17]R. M. Mazo, Ph.D. thesis, Yale University, 1955 (unpublished).
[18]A. K. Raychaudhuri and R. O. Pohl, Solid State Commun. **44**, 711 (1982).
[19]A. C. Adams, F. B. Alexander, C. D. Capio, and T. E. Smith, Electrochem. Soc. J. **128**, 1545 (1981); J. R. Holiahan, Electrochem. Soc. J. **126**, 930 (1979); G. Kaganowicz, V. S. Ban, and J. W. Robinson, J. Vac. Sci. Technol. A **2**, 1233 (1984).
[20]H. B. G. Casimir, Physica **5**, 495 (1938).
[21]J. E. VanCleve, T. Klitsner, and R. O. Pohl, in *Phonon Scattering in Condensed Matter V*, edited by A. C. Anderson and J. P. Wolfe (Springer, Berlin, 1986), p. 177.
[22]T. Klitsner, J. E. VanCleve, H. E. Fischer, and R. O. Pohl, Phys. Rev. B **38**, 7576 (1988).
[23]W. Eisenmenger, in Ref. 21, p. 204.
[24]H. Kinder, in *Physics of Phonons*, edited by T. Paszkiewicz (Springer, Berlin, 1987), p. 289.
[25]R. Maboudian, C. Carraro, D. L. Goodstein, R. M. Housley, and T. A. Tombrello, Phys. Rev. B **38**, 12190 (1988).
[26]O. Weis, in Ref. 21, p. 381.
[27]T. Klitsner and R. O. Pohl, Phys. Rev. B **34**, 6045 (1986); **36**, 6551 (1987).
[28]R. Balzer, D. S. Kupperman, and R. O. Simmons, Phys. Rev. B **4**, 3636 (1971).